Advances in Materials
2019; 8(1): 33-40
http://www.sciencepublishinggroup.com/j/am
doi: 10.11648/j.am.20190801.15
ISSN: 2327-2503 (Print); ISSN: 2327-252X (Online)

Effect of Quartz Particle Size on Sintering Behavior and Flexural Strength of Porcelain Tiles Made from Raw Materials in Uganda

William Ochen[1, 2, *], Florence Mutonyi D'ujanga[2], Bosco Oruru[2]

[1]Department of Physics, Kyambogo University, Kampala, Uganda

[2]Department of Physics, Makerere University, Kampala, Uganda

Email address:
william.ochen@yahoo.com (W. Ochen)

[*]Corresponding author

To cite this article:
William Ochen, Florence Mutonyi D'ujanga, Bosco Oruru. Effect of Quartz Particle Size on Sintering Behavior and Flexural Strength of Porcelain Tiles Made from Raw Materials in Uganda. *Advances in Materials.* Vol. 8, No. 1, 2019, pp. 33-40. doi: 10.11648/j.am.20190801.15

Received: January 18, 2019; **Accepted**: February 22, 2019; **Published**: March 18, 2019

Abstract: The presence of quartz particle size (> 45 μm) has a deleterious effect on physio-mechanical properties of porcelain tiles. The effect is due to various factors including microstructure (pore) after sintering. This study aims at investigating the effect of quartz particle size (QPS) on sintering behavior and flexural strength of porcelain tiles made from raw materials in Uganda. Samples containing fine, medium and coarse QPS were pressed at 40 MPa, fired from 1150-1350°C at a firing rate of 60°C/min, and soaked for 1 hour. The influence of QPS on linear shrinkage, water absorption and flexural strength was determined. Microstructure analysis of the fired samples was carried out using Scanning Electron Microscope (SEM), and phase identification was studies using x-ray diffraction. The SEM showed large-interconnected pores for coarse QPS, and smaller-isolated pores for fine QPS. At optimum sintering temperature, samples with fine, medium and coarse QPS had values of 0.47, 0.9 and 7.1% water absorption respectively. Pressed tiles with ≤5% water absorption are classified as group BI_a(porcelain tiles) and those > 0.5-≤3% as group BI_b suitable as floor or wall tiles (ISO 13006). Also, the average flexural strength of 33, 18 and 8 MPa was exhibited by samples with fine, medium and coarse QPS respectively. The results indicate that only samples with fine and medium QPS satisfy the requirement ≥ 35±2 MPa and > 12 MPa for floor and wall tiles respectively (ISO 13006).

Keywords: Quartz, Porcelain, Sintering, Flexural Strength

1. Introduction

A porcelain tile is a ceramic material made of kaolin clay, feldspar and quartz in the range of 40-50 wt.%, 35-45 wt.% and 10-25 wt.% respectively [1,2]. Improved physical and mechanical properties of porcelain tiles have often been at firing range of 1200-1400°C, using a fast firing schedule [3]. Typical properties of porcelain tiles are; low water absorption (≤ 0.5%) and high flexural strength (>30MPa).Today, the production of porcelain tiles has increased and the sales have improved worldwide [4,5]. The properties of porcelain tiles make them one of the top commercial products that suit both indoors and outdoors building applications. Due to the complex nature of porcelain system, there are challenges in understanding porcelains in relation to raw materials, processing conditions, phase and microstructure evolution [6].

The role played by each raw material in a porcelain system is different; kaolin reacts with feldspar and develops mullite crystals after firing. This improves on flexural strength due to interlocking of mullite needles. Feldspar begins to forms molten glass at about 980 to 1100°C, depending on its chemical composition, assisting the sintering process and enabling virtually zero water absorption [7]. Quartz promotes thermal and dimensional stability thus preventing warping. However, for glassy and vitreous materials like porcelain, the principle factor influencing flexural strength is quartz particle size [3, 6, 8, 9].

Quartz particle size has a superior effect on flexural strength compared to firing temperature and quartz content

[10]. Flexural strength is known to increases with quartz particle size in the range of 10-32 μm, this is attributed to pre-stressing effect and microstructure evolution [8, 10, 11]. According to the pre-stressing theory, the variation in thermal expansion coefficient, α, between the glassy phase (α~$3x10^{-6}$ K^{-1}) and undissolved quartz particles (α~$23x10^{-6}$ K^{-1}) in the temperature range of 20 to 700°C induces compressive stress on the glassy phase, hence improving flexural strength. Importantly, fine quartz particles dissolve at a faster rate during sintering before the coarse particles will undergo a major size reduction [3]. This changes the morphology of the pore from large, irregular and interconnected in samples with coarse quartz particle size to small, regular and isolated in samples with fine quartz particle size. Large-interconnected pores are known to act as crack transmitters other than terminators, hence reducing flexural strength.

Braganca et al. reported that flexural strength of porcelains tile with quartz particle sizes ≥ 45 μm decreases as the particle size increases. This is attributed to: (1) severe fracture around the quartz particle and within the glassy phase, due to difference in their thermal expansion coefficients, (2) the nature of pores caused by low sintering of larger quartz particles [12]. In porcelain systems, sintering curves can be used to analyze the sintering behavior of the samples. Here, the physical property (water absorption and linear shrinkage) of the samples is plotted against firing temperature [11]. Sintering curves allow establishment of optimum sintering temperature, usually corresponding to minimum water absorption or open porosity, and maximum flexural strength or linear shrinkage [1].

The aim of this article is to analyze the effect of quartz particle size on the sintering behavior and flexural strength of porcelain tiles made from Ugandan raw materials. Noteworthy, the optimum sintering temperature of samples fired from 1150-1350°C at a firing rate of 60°C/min was established. The physio-mechanical property (water absorption and flexural strength) of the samples formulated was evaluated basing on ISO 13006 standards.

2. Materials and Methods

2.1. Raw Materials

The raw materials used in this study were obtained from selected deposits in Uganda. Kaolin clay and quartz were got from Mutaka in Bushenyi District. Feldspar was got from Lunya found in Buikwe District. These deposits and their location is described in [13]. Kaolin was dry sieved using a sieve of size 80 μm. Quartz and feldspar were dry milled in a laboratory ball mill (Retsch, PM 100, German) containing twenty two steel balls as grinding medium. The mill was revolving at 350 rpm for 30 minutes, and after, pulverized feldspar was passed through 50 μm sieve. Quartz particle size was varied using different sieve sizes arranged on a sieve shaker (Retsch, AS 200, German). The mean particle sizes of 50, 90 and 200 μm were obtained, selected on the basis of [12], and classified as shown in Table 1.

Table 1. *Classification of quartz particle size.*

Quartz particle size (μm)	50	90	200
Classification	Fine	Medium	Coarse
Batch label	SQ2	SQ3	SQ4

2.2. Chemical Analysis of the Raw Materials

The chemical analysis of the raw materials was carried out by Atomic Absorption Spectrometry (Agilent, 240z/240FSAA), the concentration of the elements present was determined in parts per million (ppm), from where the percentage of their oxides was calculated. The oxides Na_2O, K_2O, Fe_2O_3, and CaO were determined by flame photometry while SiO_2 and Al_2O_3 by gravimetric method. The results of chemical analysis (Table 2) are expressed in percentage composition of the constituent oxides, and loss on ignition (LOI) was determined as a percentage of change in mass, after 2 hrs of firing at 800°C.

2.3. Preparation of Porcelain Samples

The weight proportion of the raw materials was typical of traditional porcelain; 50% kaolin, 30% feldspar and 20% quartz. Six kilograms of the mixture was homogenized in a mill for 1 hour, with plastic balls as the mixing medium. The samples were formulated by cold die pressing using a compression machine (ELE International, England) in a steel mould, and at a pressure of 40 MPa. Rectangular samples measuring 106 x 50 x 7 mm were formed from 60 g with 10 wt.% moisture content. The green samples were left to dry at room temperature for 72 hour, after which they were fired in an electric furnace (CARBOLITE, GERO, HTF 1700, German) at peak temperatures (1150-1350°C) using very fast firing schedule (60°C/min), and soaked for 1 hr. After firing, the samples were left to cool naturally in the furnace.

3. Experimental Measurements

3.1. Linear Shrinkage

The linear shrinkage of the samples was calculated using Equation (1) [14, 1]. A total of five samples were used for each peak temperature from which the average value was calculated.

$$L.S(\%)=\left[\frac{D_g - D_f}{D_g}\right]x100 \quad (1)$$

where D_g and D_f are dimensions in millimeters of the dry and fired samples respectively, measured using a digital venire caliper.

3.2. Water Absorption

The water absorption was measured using liquid displacement method according to Archimedes principle (ASTM C373-88). The masses of the dry samples (m_1) were measured using a digital electronic balance. The samples were then boiled in distilled water for 2 hours, and soaked for

24 hours at room temperature. After impregnation, the mass of the saturated samples (m_2) was measured. Five samples were used at every peak temperature from where the average value of water absorption was calculated. The water absorption, $WA(\%)$, calculated using Equation (2) [14, 1], expresses the relationship of the mass of water absorbed to mass of the dry samples.

$$WA\ (\%)\ = \frac{m_2 - m_1}{m_1} x100 \quad (2)$$

3.3. Flexural Strength/Modulus of Rupture (MOR)

The flexural strength of the samples was determined by three point loading method (using AMETEK, LLOYD INSTRUMENT, UK). The span length (L) considered in the measurement was 100 mm. A loading force (F), at 0.5 mms^{-1} was directed to the centre of the samples, and upon breaking of the test sample its value was noted. A total of seven samples were considered at every peak temperature from which the average value of MOR was calculated using Equation (3) [15].

$$MOR = \frac{3FL}{2bt^2} \quad (3)$$

where b and t are breadth and thickness of the samples respectively, measured using a digital venire caliper in millimeters.

3.4. Microstructure and Phase Analysis

The microstructures of the samples at optimum sintering temperature were characterized using CARL ZEISS Scanning Electron Microscope (SEM), EVO MA 10. Sectioned and polished specimens of the fired samples were used for the investigation. The specimens were polished, cleaned and dried. Thereafter, they were dipped in 40% concentrated hydrochloric acid for 25 s, cleaned, dried and studied using CARL ZEISS instrument. The cleaning procedures given to all specimens before examination included washing in water and alcohol before drying.

The crystalline phases in the fired porcelain samples were determined by X-ray diffraction using an X'pert PROPANalytical X-ray diffractometer, PW 3050/60, with Ni-filtered K_α Cu-radiation generated by a 40 kV acceleration voltage and a 40 mA anode current. Pulverized specimens were scanned from 10 to 90° operating the equipment at a 2θ scan-speed of 0.5 sec/step and a 2θ step size of 0.02°. The X-ray peaks of the different phases were identified with High Score software.

4. Results and Discussions

4.1. Chemical Composition

Chemical analysis was done on all the raw materials used in the study, and results are given in Table 2. The raw materials were got from selected deposits and processed for chemical analysis with no additives.

Table 2. *Chemical composition (%) of the raw materials.*

Oxide	Composition of raw materials (%)		
	Kaolin	**Feldspar**	**Quartz**
SiO_2	53.41	62.82	99.59
Al_2O_3	35.64	17.23	-------
Fe_2O_3	0.03	0.14	0.04
Na_2O	0.04	0.30	0.04
K_2O	0.01	4.23	0.02
Ca O	0.28	0.29	0.39
Others	0.63	17.5	------
LOI	9.96	1.49	0.39

The chemical composition of kaolin, quartz and feldspar shows that they are of common type used in formulation of porcelain tiles [1]. The chemical composition of quartz reveals that it is composed of pure SiO_2 (99.59%). Further, kaolin contains average and recommendable amount of SiO_2 and Al_2O_3 at 53.41 and 35.64% respectively. The chemical analysis also shows that potash feldspar is the major fluxing oxide composed of mainly SiO_2, its K_2O value is 4.23% compared to other flux oxides Na_2O and CaO with 0.30 and 0.29% respectively. However, the percentage of K_2O is low in this study as compared to that reported by other workers [1, 13, 16]. This is attributed to processing technique, as feldspar was not washed or soated to remove impurities like quartz; feldspar was milled as got from the deposit and tested for chemical composition. The flux oxide plays a significant role towards densification, by forming a vitreous phase that blocks the open pores present in the microstructure. On the same note, they contribute towards phase transformation, mullite formation where their presence in the porcelain body enhances mechanical strength [17]. The lower flux oxide probably explains the high optimum sintering temperature of 1300°C exhibited in this study, similar work reported a value of 1250°C [13]. The chemical analysis (Table 2) further shows that the percentage of Fe_2O_3 is low in all the raw materials. This explains the whiteness of the fired samples. Iron III oxide is an impurity that affects the color of samples, and causes bloating due to escape of entrapped gases [18]. Other oxides such as P_2O_3, MgO, MnO and TiO_2 were not analyzed, similar work reported negligible amount [13]. Also, no literature known to the researcher attributes their role on flexural strength or water absorption.

4.2. Linear Shrinkage

The shrinkage behavior of porcelain products during sintering is important, because it allows controlling the dimensions of the final product [4]. The shrinkage of the samples was plotted against the firing temperature. Figure 1 displays a general increase in shrinkage as temperature raises from 1150-1300°C. The results show a same value of shrinkage (0.8%) of all the batches at 1150°C, and for batches SQ2 and SQ3 (4.6%) at 1200°C. There is a further increase in shrinkage at 1300°C, and slight decline at 1350°C for SQ2 and SQ3. Batch SQ4 exhibited shrinkage of 2.8% at

1200°C, firing further yielded no change in the shrinkage. The maximum shrinkage for all batches (7.9%) was exhibited by SQ2. Noteworthy, the shrinkage of the samples decreases with increasing quartz particle size (Figure 1inset).The discussions in this study were focused on batches with fine and coarse quartz particle size due to distinct nature of their results.

The increase in shrinkage with temperature is attributed to the reduction in particle size as they approach fusion. The particles melt as temperature increase further and the viscosity of the melted glassy phase formed decreases as temperature is raised. Therefore, when the body cools, particles pull together leading to increase in shrinkage [19]. The high shrinkage means that more thermal changes occurred within the raw materials, and this behavior is fostered by increasing temperature [4]. However, above 1300°C, as the melted glassy substance becomes less viscous, bubble begin to form due to escape of entrapped gasses, and shrinkage of the samples reduces due to increase in total porosity of the samples. In most cases bubbles develop when samples are fired beyond their optimum temperature. This will be discussed later in microstructure observation.

The shrinkage of the samples reduced as the size of quartz particles increased. This behavior is typical of porcelain materials [20]. During sintering, the presence of fine quartz particles increases the amount of silica content in the liquid phase, which fills the pores and promotes densification of the particles. Fine quartz particles dissolve faster because more of their surface area is exposed to the liquid phase emanating from feldspar [8], fostering shrinkage. Subsequently, low shrinkage noticed by using coarse quartz particles is attributed to low rate of dissolution, which reduces the amount of glassy phase therefore creating large pores in the microstructure [21]. At 1150°C no variation in shrinkage is noticed by different batches, probably because quartz dissolution had not started yet.

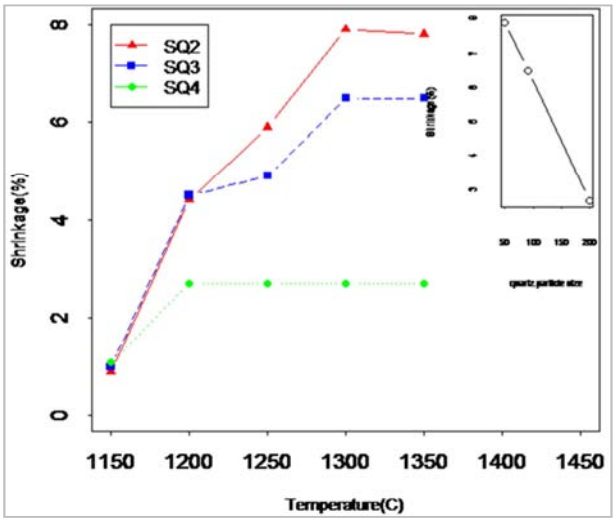

Figure 1. *Variation of shrinkage with temperature, and decline of shrinkage with quartz particle size (inset).*

4.3. Water Absorption

Water absorption defines the durability and the class to which the final porcelain tile belongs [4]. The water absorption reduced with increase in firing temperature from 1150-1300°C, and at 1350°C, no significant change is observed (Figure 2).This trend is typical of porcelain materials [3]. Batches SQ2 and SQ3 exhibited almost the same behavior at all temperatures, while SQ4 had higher values ranging from 6 to 13%. Figure 2 (inset) shows how water absorption varies with quartz particle size at 1300°C. It is observed that water absorption increases with quartz particle size. At 1300°C, SQ2 had a value of 0.47% which is slightly less than 0.5%. According to ISO 13006 standards, these type of ceramic materials are classified as porcelain tiles (group BI_a), and recommended for use as floor tiles [4]. International standards (ISO 13006) further classifies pressed tiles with $> 0.5 - \leq 3\%$ water absorption as group BI_b, SQ3 with 0.9% water absorption lies in this range and is also recommended for use as tiles. However, tiles with 6-10% water absorption are classified as group BIII, and SQ4 with 7.1% is within this range. These are not suitable for use as floor tiles [22].

The water absorption decreases with increase in firing temperature. This observation is a result of good densification of the samples [9]. At about 1100°C, K-feldspar starts melting to form a liquid phase that surrounds the particles [2]. The capillary pressure created at the contact points binds the particles closer while altering pore size and shape, hence lowering water absorption. Further increase in temperature reduces the viscosity of the liquid substance formed, contributing to decrease in pore size and further reduction in water absorption [23].

Batches with fine quartz particle size distribution exhibited lower water absorption than coarse particles. This is because raising the quartz particle size leads to larger quantities of undissolved quartz grains due to low sintering thereby increasing the size of the pores [24]. It is known that, due to non plastic nature of quartz, it disperses in the green body containing voids between clay platelets. After sintering, pores of the size related to the non plastic material are formed. This connects well with the raise in water absorption as the quartz particle size was increased. On the other hand, fine quartz particles melt away easily, increasing the glassy phase, and forming smaller, regular and isolated pores in the microstructure. This signifies high degree of liquid phase sintering, and densification. Preferably explaining low water absorption exhibited, similar results were obtained by [12].

In this study, the sintering behavior of the fired samples was evaluated by linear shrinkage and water absorption [1]. The optimum sintering temperature was considered when water absorption reached a minimum value, tending to zero, and simultaneously linear shrinkage was maximum. This was exhibited at a peak temperature of 1300°C. However, at 1350°C bubbles started to appear in the microstructure of the fired samples hence affecting their properties.

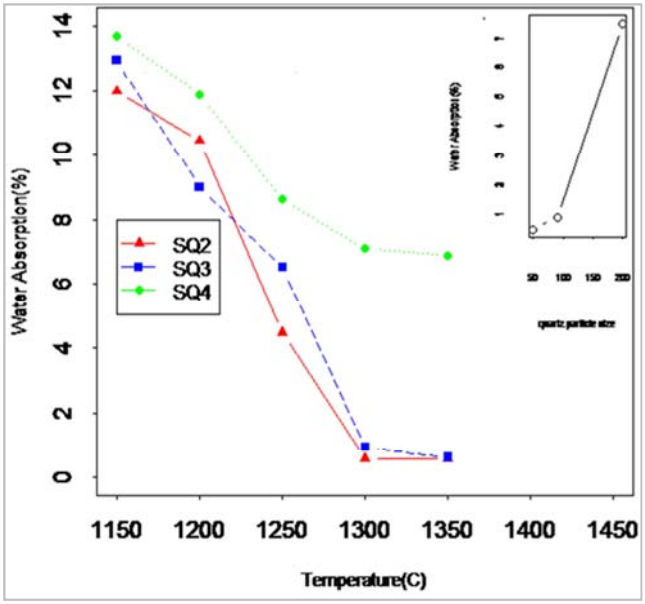

Figure 2. *Variation of water absorption with temperature, and increase of water absorption with Quartz Particle Size at 1300°C (inset).*

4.4. Flexural Strength/Modulus of Rupture (MOR)

The flexural strength of the samples containing different quartz particle sizes, fired at different temperature is given in Figure 3. The results illustrate that the flexural strength increases with firing temperature (1150-1300°C), and decreases when the quartz particle size is increased (Figure 3 inset). At 1300°C, the average flexural strength values of SQ2 and SQ3 particles are 33 MPa and 18 MPa respectively. Also, the samples with coarse quartz particle size (SQ4) presented the lowest flexural strength of 8Mpa. The results indicate that SQ2 satisfies the requirement $\geq 35 \pm 2$ MPa for floor tiles (ISO 13006), and batch SQ3 satisfies the requirement >12 MPa for wall tiles [4]. The coarse quartz size samples did not meet any required specifications.

The increase in flexural strength with temperature is attributed to the reactions that occur during the sintering process, such as; elimination of pores and formation of crystalline phases like mullite [23]. Increasing temperature eliminated open pores by viscous flow, which is controlled by melt viscosity. The melt viscosity is directly related to the particle size of quartz, a dense microstructure is achieved by decreasing the quartz particle size. Since the powers of fine sized quartz particles are higher than those of coarse quartz particles, their mobility is also higher thus they can react easily and increase the speed of sintering [25]. Another important issue is particle parking density after pressing; this is controlled by particle size of the material being processed. Fine quartz particles have a higher packing density than coarse particles. The diffusion distance of the particles can be shortened to increase sintering speed with dense parking. As a result the flexural strength values of the fired samples increases.

On the other hand, the increase in flexural strength is also attributed to mullite content. According to mullite hypothesis [10], mullite crystals act as a re-enforcement to the glassy phase. The mullite content is enhanced by fine size of the quartz particles [9]. Recently, Güngör (2018) investigated the influence of quartz particle size on the mechanical strength of porcelain. The author reported that the amounts of secondary mullite crystals are increased by decreasing the particle size of quartz and increasing the temperature. In conclusion, flexural strength is improved by reducing the size of quartz particles, because the mullite content is improved at elevated temperature.

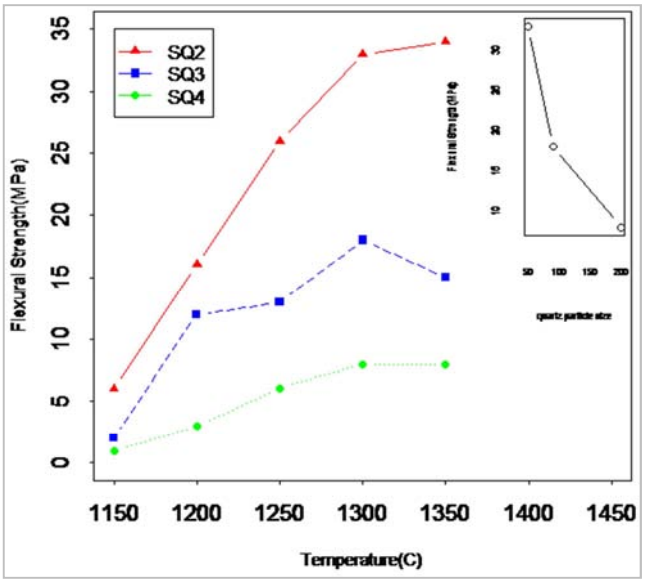

Figure 3. *Variation of flexural strength with temperature, and decrease of flexural strength with quartz particle size at 1300°C (inset).*

4.5. Microstructure and Phase Analysis

The Scanning Electron Microscope (SEM) micrographs of samples fired at 1300°C with fine (SQ2) and coarse (SQ4) quartz particle sizes are represented in (Figure 4). Comparing micrographs, it is observed that quartz particle size influences the microstructure evolution of the final products. The sintered body with coarse quartz particle size (Figure 4b) shows a rough and granular texture. This probably shows undissolved quartz grains. As a result of low sintering, large pores in the range of 11 to 34 µm were formed by coarse particles, relating to high water absorption (7.1%) and low flexural strength (8 MPa). The samples with fine quartz particles exhibited a higher degree of glassy phase forming a smooth surface, compacted texture and dense microstructure (Figure 4a), relating to low water absorption (0.47%) and high flexural strength (33 MPa). The small pores of size 3-10 µm formed by fine quartz particles, indicates high degree of liquid formation since fine quartz particles are known to dissolve faster [3].

Similarly, due to high viscosity of the glassy phase by coarse quartz particles, there is a delay in the homogenization of the texture/particles, this may be the reason for large, irregular and interconnected nature of the pores [27] (Figure 4d). Mostly, this signifies low degree of liquid formation probably due to a very high sintering rate (60°C/min) used in

this study. Interconnected pores are detrimental because they facilitate crack propagation thereby decreasing flexural strength [8,16], relating to 8 MPa obtained in this study. Likewise, spherical and isolated pores in samples with fine quartz particles (Figure 4c) relates to densification (<0.5% water absorption). This characterizes the final stage of sintering [16]. Isolated pores are known to act as termination points for crack propagation hence enhancing flexural strength.

The slight decline in flexural strength and shrinkage of samples fired beyond 1300°C is attributed to bloating (Figure 4e). Expulsion of gasses (bloating) occurs in the liquid phase at higher temperature leading to increase in total porosity [23] or water absorption in this case. The origin of bloating in the liquid substance can be associated with the loss of the hydroxyl group in the kaolinitic mineral ($Al_2O_3.2Si\,O_2.2H_2O$) and more severely during the release of oxygen due to the decomposition of Fe_2O_3 to Fe_3O_4 [8].However, it is reported that bloating is not a heating rate effect, but it occurs when samples are fired beyond the optimum temperature [27].

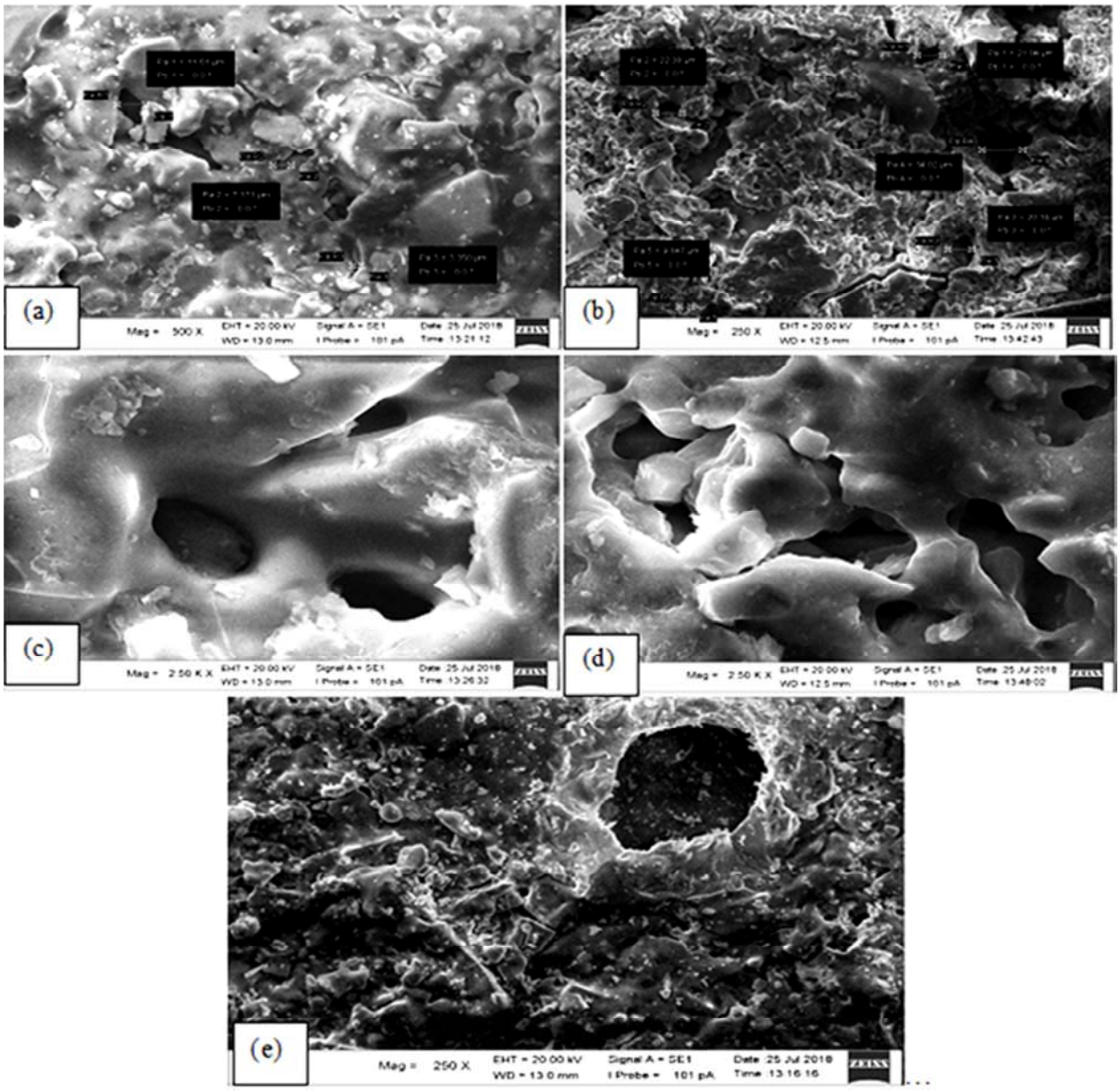

Figure 4. *SEM micrographs of samples: (a) smooth texture by fine quartz at 1300°C; (b) rough texture by coarse quartz at 1300°C; (c) isolated pores by fine quartz at 1300°C; (d) interconnected pores by coarse quartz at 1300°C and (e) bloating at 1350°C.*

X-ray diffractograms of samples containing fine (a), medium (b) and coarse (c) quartz particle size, fired at 1300°C are illustrated in Figure 5. It can be noted that the principle crystalline phase present in the samples is quartz (Q), represented by the highest intensity peak at $2\theta{\sim}25^0$. It can be seen that the intensity of the quartz peaks increases in parallel with the increase of the quartz particle size, which indicates low dissolution of coarse quartz particles and high dissolution for fine particles [9]. Similarly, the intensity of mullite (M) peaks increases with decreasing quartz particle

size (Figure 5), implying that samples with fine quartz particle size exhibited a higher population of mullite crystals than others hence improving their flexural strength.

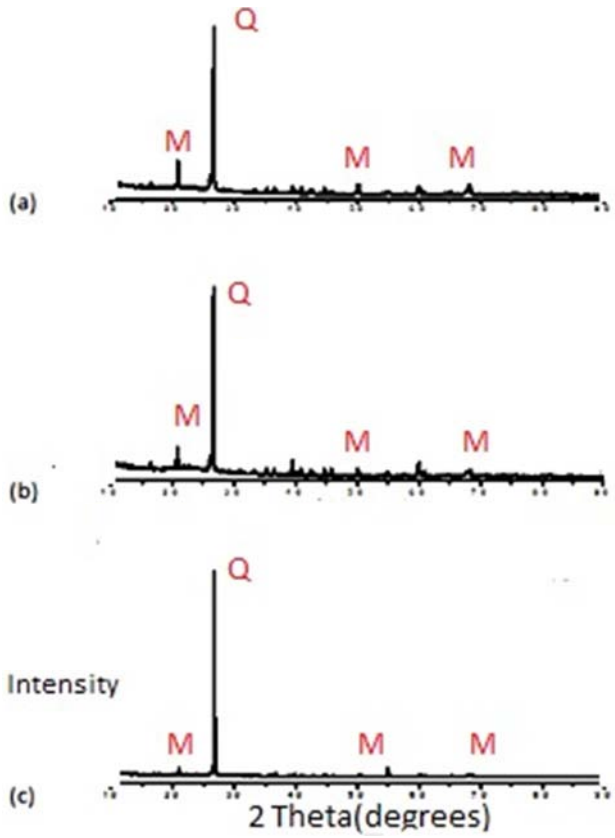

Figure 5. *XRD diffractograms of samples at 1300°C: (a) fine ;(b) medium and (c) coarse quartz particle sizes.*

5. Conclusion

In this study, the effect of using different quartz particle sizes on the sintering behavior and flexural strength of porcelain tiles has been investigated. The SEM analysis revealed isolated and spherical pores for samples with fine quartz particle sizes. However, irregular and interconnected pores were observed in samples containing coarse quartz particle sizes. This is responsible for the increase in water absorption and decrease in flexural strength. At optimum sintering temperature, the flexural strength of the samples is 8, 18 and 33 MPa for coarse, medium and fine quartz particle sizes respectively. The standards (ISO 13006) recommends tiles with water absorption $\geq 35 \pm 2$ MPa as floor tiles and those with >12 MPa as wall tiles. On the same note, water absorption exhibited by fine, medium and coarse quartz particle sizes is 0.47, 0.9 and 7.1% respectively. International standards further classify tiles whose water absorption is $\leq 0.5\,\%$ as group BI_a (also known as porcelain tiles). Tiles with water absorption of $> 0.5 - \leq 3\%$ are categorized as group BI_b. Both cases are acceptable as floor or wall tiles. .However, samples with coarse quartz particle size exhibited properties (water absorption and flexural strength) that did not meet the required specifications for both floor or wall tiles.

Acknowledgements

This research was supported by Deutscher Akademischer Austauschdient German Academic Exchange Service (DAAD).

References

[1] J. Martín-Márquez, J. M. Rincón, and M. Romero, “Effect of firing temperature on sintering of porcelain stoneware tiles,” Ceram. Int., vol. 34, 2008, pp. 1867–1873.

[2] V. Sanz, A. Moreno, and E. Sa, “Porcelain tile : Almost 30 years of steady scientific-technological evolution,”Ceram. Int.,vol. 36, 2010, pp. 831–845.

[3] O. Turkmen, A. Kucuk, and S. Akpinar, “Effect of wollastonite addition on sintering of hard porcelain,” Ceram. Int., vol. 41, 2015, pp. 5505–5512.

[4] O. R. Njindam, D. Njoya, J. R. Mache, M. Mouafon, A. Messan, and D. Njopwouo, “Effect of glass powder on the technological properties and microstructure of clay mixture for porcelain stoneware tiles manufacture,” Constr. Build. Mater., vol. 170, 2018, pp. 512–519.

[5] M. F. Abadir, E. H. Sallam, and I. M. Bakr, “Preparation of porcelain tiles from Egyptian raw materials,” Ceram. Int., vol. 28, 2002,, pp. 303–310.

[6] K. Dana, S. Das, and S. K. Das, “Effect of substitution of fly ash for quartz in triaxial kaolin-quartz-feldspar system,” J. Eur. Ceram. Soc., vol. 24, 2004, pp. 3169–3175.

[7] W. M. Cam and U. Senapati, “Porcelain-Raw Materials, Processing, Phase Evolution, and Mechanical Behavior,” J. Am. Ceram. Soc., vol. 81, 1998, pp 3-20.

[8] Y. Kobayashi, O. Ohira, Y. Ohashi, and E. Kato, “Effect of Firing Temperature on Bending Strength of Porcelains for Tableware,” J. Am. Ceram. Soc., vol. 75, 1992, pp. 1801–1806.

[9] L. Boussouf, F. Zehani, Y. Khenioui, and N. Boutaoui, “Effect of Amount and Size of Quartz on Mechanical and Dielectric Properties of Electrical Porcelain,” Trans. Indian Ceram. Soc., vol. 77, 2018, pp. 132–137, 2018.

[10] G. Stathis, A. Ekonomakou, C. J. Stournaras, and C. Ftikos, “Effect of firing conditions, filler grain size and quartz content on bending strength and physical properties of sanitaryware porcelain,” J. Eur. Ceram. Soc., vol. 24, 2004, pp. 2357–2366.

[11] O. I. Ece and Z. E. Nakagawa, “Bending strength of porcelains,” Ceram. Int., vol. 28, 2002, pp. 131–140.

[12] S. I. WARSHAW and R. SEIDER, “Comparison of Strength of Triaxial Porcelains Containing Alumina and Silica,” J. Am. Ceram. Soc., vol. 50, 1967, pp. 337–343.

[13] P. W. Olupot, S. Jonsson, and J. K. Byaruhanga, “Development and characterisation of triaxial electrical porcelains from Ugandan ceramic minerals,” Ceram. Int., vol. 36, 2010, pp. 1455–1461.

[14] O. S. Mahdi, “Study the Influence of Sintering on the Properties of Porcelain Stoneware Tiles,” vol. 13, 2018, pp. 3248–3254.

[15] V. G. Lee and T. H. Yeh, “Sintering effects on the development of mechanical properties of fired clay ceramics,” Mater. Sci. Eng. A, vol. 485, 2008, pp. 5–13.

[16] J. L. Amorós, M. J. Orts, S. Mestre, J. Garcia-Ten, and C. Feliu, "Porous single-fired wall tile bodies: Influence of quartz particle size on tile properties," J. Eur. Ceram. Soc., vol. 30, 2010, pp. 17–28.

[17] Y. Iqbal and W. E. Lee, "Microstructural evolution in triaxial porcelain.," J. Am. Ceram. Soc.vol. 27, 2000, pp. 3121–3127.

[18] S. Kitouni and A. Harabi, "Sintering and mechanical properties of porcelains prepared from algerian raw materials," Cerâmica, vol. 57, 2011, pp. 453–460.

[19] A. Salem, S. H. Jazayeri, E. Rastelli, and G. Timellini, "Thermochimica Acta Kinetic model for isothermal sintering of porcelain stoneware body in presence of nepheline syenite," Thermochim. Acta, vol. 503–504, 2010. pp. 1–7.

[20] G. P. Souza, P. F. Messer, and W. E. Lee, "Effect of varying quartz particle size and firing atmosphere on densification of Brazilian clay-based stoneware," J. Am. Ceram. Soc., vol. 89,2006, pp. 1993–2002.

[21] S. R. Bragança and C. P. Bergmann, "Effect of Quartz of Fine Particle Size on Porcelain Properties," Mater. Sci. Forum, vol. 530–531, 2006, pp. 493–498.

[22] M. Romero and J. M. Pérez, "Relation between the microstructure and technological properties of porcelain stoneware . A review," Mater. construcción, vol. 65, 2015, pp. 1–19.

[23] G. Gralik,L. Chinelatto,S. Chinelatto, and P. Grossa, "Effect of different sources of alumina on the microstructure and mechanical properties of the triaxial porcelain "Ceramica, vol. 60., 2014, pp 471–481.

[24] M. F. Quereda and M. J. Ib, "Porcelain tile microstructure : implications for polishability,"J. Eur. Ceram. Soc. vol. 26, 2006, pp. 1035–1042.

[25] F. Güngör and N. Ay, "The effect of particle size of body components on the processing parameters of semi transparent porcelain," Ceram. Int., vol. 44, 2018, pp. 10611–10620.

[26] T. K. Mukhopadhyay, S. Ghosh, S. Ghatak, and H. S. Maiti, "Effect of pyrophyllite on vitrification and on physical properties of triaxial porcelain," Ceram. Int., vol. 32, 2006, pp. 871–876.

[27] W. Lerdprom, R. K. Chinnam, D. D. Jayaseelan, and W. E. Lee, "Porcelain production by direct sintering," J.Eur. Ceram. Soc., vol. 36, 2016, pp. 4319–4325.